International Journal of Bifurcation and Chaos, Vol. 20, No. 6 (2010) 1751–1760

DOI: 10.1142/S0218127410026800

PREDICTING THE SYNCHRONIZATION OF A NETWORK OF ELECTRONIC REPRESSILATORS

ISAO T. TOKUDA
School of Information Science,
Japan Advanced Institute of Science and Technology,
Ishikawa 923-1292, Japan

ALEXANDRE WAGEMAKERS and MIGUEL A. F. SANJUÁN
Nonlinear Dynamics, Chaos and Complex Systems Group,
Departamento de Física, Universidad Rey Juan Carlos,
Tulipán s/n, 28933 Móstoles, Madrid, Spain

Received November 1, 2008; Revised July 17, 2009

Synchronization of coupled oscillators is by now a very well studied subject. A large number of analytical and computational tools are available for the treatment of experimental results. This article focuses on a method recently proposed to construct a phase model from experimental data. The advantage of this method is that it extracts a phase model in a noninvasive manner without any prior knowledge of the experimental system. The aim of the present research is to apply this methodology to a network of electronic genetic oscillators. These electronic circuits mimic the dynamics of a synthetic genetic oscillator, called "repressilator", which is capable of synthesizing autonomous biological rhythms. The obtained phase model is shown to be capable of recovering the route leading to synchronization of genetic oscillators. The predicted onset point of synchronization agrees quite well with the experiment. This encourages further application of the present method to synthetic biological systems.

Keywords: Synchronization; phase oscillator; genetic networks.

1. Introduction

The synchronization of coupled oscillators has received much attention in the past few years within the context of nonlinear dynamics. Since oscillators are ubiquitous around us, this explains the large volume of literature dedicated to this subject. Among the long list of examples it is worth citing coupled systems, which spontaneously synchronize such as neurons [Elson *et al.*, 1998], menstrual synchrony among women [McClintock, 1971], and genetic clocks [Yamaguchi *et al.*, 2003]. Synchronization plays an important role also in biological rhythms such as the circadian clock located at the suprachiasmatic nucleus (SCN) of the hypothalamous in mammals. The SCN is composed of $\sim 10{,}000$ neurons, each of which is a self-sustained oscillator with a varied frequency. Through the mutual coupling, the SCN neurons are synchronized to form the circadian rhythm. It is therefore indispensable to study the biological rhythm under the framework of coupled oscillators.

In the study of coupled oscillators, one of the most standard modeling approaches is the phase equation modeling, which can be applied to weakly coupled limit cycle oscillators [Kuramoto, 1984]. Because of its very simple mathematical expression, the phase modeling technique has been applied

to a variety of systems including the biological rhythms [Winfree, 1980; Galan *et al.*, 2005; Kori & Mikhailov, 2004]. However, an important problem of constructing the phase models from experimental biological data still remains open. Hence, the present article aims at constructing a phase model from an experimental system that mimics the dynamics of a genetic oscillator. This genetic oscillator, called the "repressilator", has been conceived and built in laboratory from scratch [Elowitz & Leibler, 2000]. The experiment shows a periodic evolution of a protein level in bacteria genetically manipulated. The underlying dynamics of this oscillator can be described by a very simple mathematical model based on ordinary differential equations. This equation can be simulated in many ways and we have proposed an analog simulation with electronic circuits [Wagemakers *et al.*, 2006]. Furthermore, we have demonstrated that the synchronization could be achieved within a set of oscillators with a global coupling between the units. This synchrony, which has been described theoretically [García-Ojalvo *et al.*, 2004], has not yet been observed in a synthetic biological system. Hence, our electronic genetic network provides an important initial step towards the analysis of real biological systems. In a biological experimental setup, the only variable accessible for observation is a fluorescent marker that reflects the state of an internal variable. The time lapse fluorescence microscopy is a recent technique that allows the recording of a time series of an evolving process in a cell population. The time series analysis presented is particularly well suited for this experimental setup since it is noninvasive and uses the fluorescence as the state of a phase oscillator.

The method of constructing the phase model is based on an approach [Tokuda *et al.*, 2007], recently developed to extract phase models from multivariate time series. This approach has an important practical advantage that no prior knowledge of the underlying dynamics is required. Compared with the conventional techniques [Kuramoto, 1984; Sakaguchi *et al.*, 1987; Kiss *et al.*, 2005; Galan *et al.*, 2005; Miyazaki *et al.*, 2006], which are rather invasive in the sense that a perturbation is applied to an isolated oscillator or two coupled oscillators should be extracted from a population of oscillators, the present approach utilizes only a set of time series recorded from all the units. This noninvasive property can be a great advantage especially for the application to biological systems. First, natural frequencies of the units as well as interaction function between the units are estimated by the multiple shooting technique. Then, the estimated phase model can be simulated for a different coupling value to study the dependence of synchronization on the coupling strength. One of the highlights of the estimation technique is its ability to reconstruct the route to synchronization from only a single time series of the experimental setup in a weak coupling configuration. This single data set is shown to be sufficient to predict the onset point of full synchronization in the experimental system.

2. The Repressilator Model

The original repressilator model is founded on a synthetic biology experiment first published in [Elowitz & Leibler, 2000]. The authors constructed an oscillator with different genes, which are present in the bacteria *E. Coli* and made them interact artificially. It is composed of three different genes which produce proteins capable of interacting with other genes by inhibiting their protein synthesis. The structure of the repressilator is the following: Gene 1 produces a protein that silences gene 2, gene 2 represses gene 3 and gene 3 inhibits gene 1. This closed chain of inhibitions is called the repressilator. It has been demonstrated experimentally that sustained oscillations do exist for the repressilator. The dynamics of this system can be expressed by a simple mathematical model of coupled ordinary differential equations. In the following set of equations, each dynamical variable p_i represents the concentration of a protein produced by one of the genes:

$$\frac{dp_1}{dt} = -\gamma_{p1} p_1 + \frac{\alpha_1}{1 + \left(\frac{p_3}{K_0}\right)^n} \tag{1}$$

$$\frac{dp_2}{dt} = -\gamma_{p2} p_2 + \frac{\alpha_2}{1 + \left(\frac{p_1}{K_0}\right)^n} \tag{2}$$

$$\frac{dp_3}{dt} = -\gamma_{p3} p_3 + \frac{\alpha_3}{1 + \left(\frac{p_2}{K_0}\right)^n}. \tag{3}$$

The parameter γ_{pi} holds for the protein mean life, the parameter α_i is the protein production rate and K_0 and n are related to the strength of the repression of the specific protein. This repressilator model can be simulated with a very simple

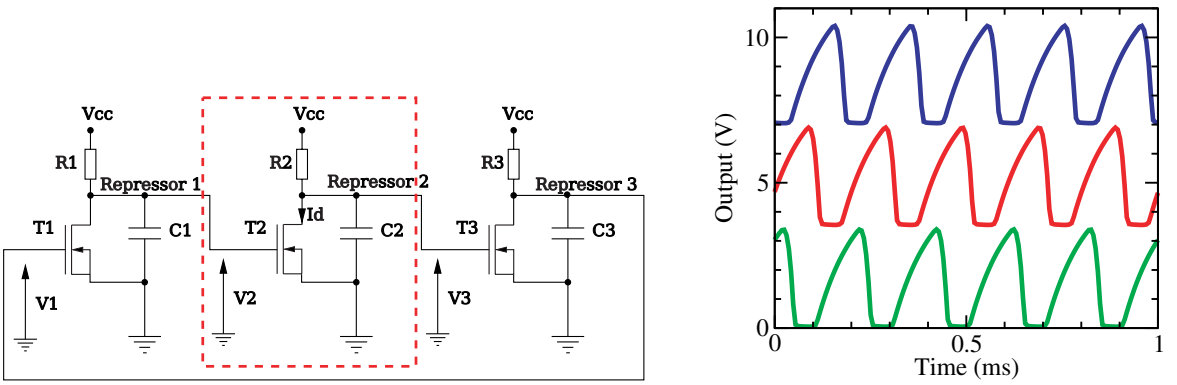

(a) (b)

Fig. 1. (a) Basic circuit of the repressilator with a MOSFET transistor and discrete linear components. (b) Typical time series of the three voltages V_1, V_2 and V_3.

analog electronic circuit [Wagemakers *et al.*, 2006]. The circuits reflect the most important aspect of the dynamics, which is the mutual repression of each gene. The basic circuit is composed of three MOSFET transistors which actuates as controllable switches as it can be seen in Fig. 1(a). In the absence of tension on the gate of the transistor i, the voltage V_i increases until it reaches a threshold and shuts down the tension V_{i+1}. It reproduces the circular inhibition of the repressilator perfectly as it can be seen in the time series of Fig. 1(b).

The protein concentration of each bacteria oscillates individually with its own phase and frequency without any kind of observable global behavior. To explore the effects of the synchronization on a colony of repressilators, several units have been coupled with a simple resistor to a common point in the configuration shown in Fig. 2. The synchronization of the different units is possible to achieve with the variation of the coupling of the resistance R_c. The level of coupling needed to synchronize the system will be detailed in Sec. 3.

In order to obtain the prediction with the numerical method, we need to describe in some detail a model of the circuit of Fig. 1. First, it is convenient to analyze the behavior of a single cell to understand the complete model. The basic unit of the circuit representing the dynamics of the repressilator can be viewed in Fig. 1 in the dashed box. The core of the model is a MOSFET circuit which behaves as a switch controlled by the gate voltage. Based on the MOSFET enhancement n-channel model, we have the following expression for the drain current i_d:

$$i_d(V_i, V_{i-1}) = \begin{cases} 0 & \text{for } V_{i-1} < V_{\text{th}} \\ K(2V_i(V_{i-1} - V_{\text{th}}) - V_i^2) & \text{for } 0 < V_i < V_{i-1} - V_{\text{th}} \\ K(V_{i-1} - V_{\text{th}})^2 & \text{for } 0 < V_{i-1} - V_{\text{th}} < V_i, \end{cases} \tag{4}$$

with K and V_{th} two parameters depending on the considered MOSFET model. Other models can also be used for the drain current. A simpler model can be approximated in the form of a continuous function:

$$id(V_i, V_{i-1}) = K(V_{i-1} - V_{\text{th}})^2 \left(\frac{V_i}{V_i + V_{i-1} - V_{\text{th}}} \right) \times \left(\frac{\left(\frac{V_{i-1}}{V_{\text{th}}} \right)^n}{1 + \left(\frac{V_{i-1}}{V_{\text{th}}} \right)^n} \right).$$

The equation that rules the dynamics of one basic cell can be written as:

$$C_i \frac{dV_i}{dt} = \frac{(V_{cc} - V_i)}{R_i} - i_d(V_i, V_{i-1}), \tag{5}$$

which is the sum of the currents in the transistor C_i. However, to simplify the analysis a simpler model can be obtained after some assumptions. The set of equations is reduced to:

$$R_2 C_2 \frac{dV_2}{dt} = -V_2 + V_{cc} f(V_1) + \alpha, \tag{6}$$

$$R_3 C_3 \frac{dV_3}{dt} = -V_3 + V_{cc} f(V_2) + \alpha, \tag{7}$$

$$R_1 C_1 \frac{dV_1}{dt} = -V_1 + V_{cc} f(V_3) + \alpha, \tag{8}$$

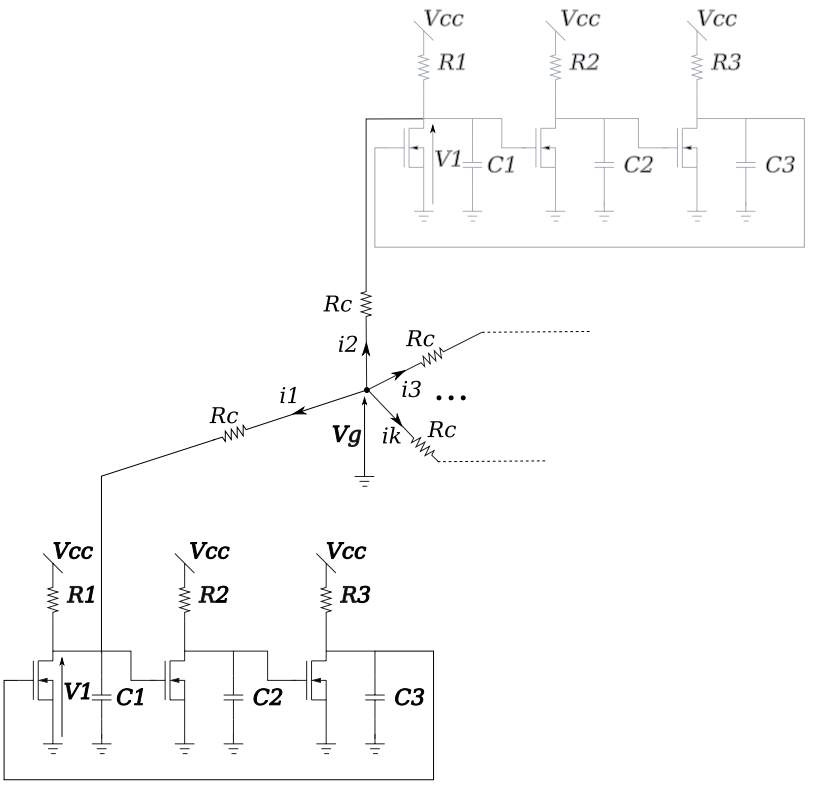

Fig. 2. Schematics of the coupled system, the variable V_1 is connected to a common point through a resistor R_c.

with $f(x) = 1/(1 + (x/V_{\text{th}})^n)$. This expression is similar to the model of the repressilator in Eqs. (1)–(3).

The coupling between the units is achieved through a common resistor to all the circuits as shown in Fig. 2. The voltage V_1 of each circuit is connected to a common point through a resistor R_c. We obtain in this way a global coupling of the system. In order to obtain the equation of the coupled circuit, we have to consider first the voltage V_g of the common point where all the resistors R_c are connected. The current flowing from this point to one of the voltage V_1 of the repressilator n is:

$$i_n = \frac{(V_g - V_1^n)}{R_C}, \tag{9}$$

with V_1^n the voltage V_1 of the circuit n. On the other hand, we have the sum of all the currents at this point:

$$\sum_{n=1}^{N} i_n = 0, \tag{10}$$

which leads to:

$$\sum_{n=1}^{N} (V_g - V_1^n) = 0. \tag{11}$$

We deduce that V_g is the mean of all the voltages:

$$V_g = \frac{1}{N} \sum_{n=1}^{N} V_1^n. \tag{12}$$

It is now straightforward to deduce the set of ODE's of the coupled system:

$$R_2 C_2 \frac{dV_2}{dt} = -V_2 + V_{cc} f(V_1) + \alpha, \tag{13}$$

$$R_3 C_3 \frac{dV_3}{dt} = -V_3 + V_{cc} f(V_2) + \alpha, \tag{14}$$

$$R_1 C_1 \frac{dV_1}{dt} = -V_1 + V_{cc} f(V_3) + \alpha + R_1 \frac{1}{R_c} \frac{1}{N} \sum_{n=0}^{N} (V_1^n - V_1). \tag{15}$$

The parameters used in the experiments are:

- $R_1 = R_2 = R_3 = 1\,\text{k}\Omega$ with a variability of 10%
- $C_1 = C_2 = C_3 = 1\,\mu\text{F}$ with a variability of 10%
- $V_{cc} = 3V$
- $V_{th} = 2.3\text{V}$ with a variability of 10%

3. Problem and Method

The coupled system described in the previous section can be synchronized depending on the coupling

value R_c. In this section, we expose the method that will give us the coupling value necessary to obtain this synchronization.

Consider a system of N weakly coupled nearly identical limit cycle oscillators:

$$\dot{x}_i = F_i(x_i) + \frac{C}{N}\sum_{j\neq i}^{N} G(x_i, x_j), \tag{16}$$

where x_i and F_i $(i = 1, 2, \ldots, N)$ represent state variables and the dynamics of the ith oscillator, C and G represent the coupling constant and the interaction function between the ith and jth oscillators. Our assumption is that in an isolated condition $(C = 0)$, i.e. uncoupled oscillators, each oscillator F_i gives rise to a stable limit cycle with similar natural frequencies ω_i. Then the phase reduction theory [Kuramoto, 1984] states that for weak uniform coupling C, the network dynamics can be reduced to the phase equations:

$$\dot{\theta}_i = \omega_i + \frac{C}{N}\sum_{j=1}^{N} H(\theta_j - \theta_i) \tag{17}$$

(θ_i: phase of ith oscillator; H: interaction function). As a reminder, we assume that a simultaneous measurement of all oscillators is made as $\{x_i(n\Delta t) : n = 1, \ldots, M\}_{i=1}^{N}$ (Δt: sampling time).

Our goal is to infer the phase equations from the measurement data under the conditions that:

(1) the underlying dynamics (16) are unknown,
(2) the coupling constant C associated with the measured data is taken from a nonsynchronous regime, and
(3) the coupling type is known to be uniform and an all-to-all connection.

The estimation does not require an *a priori* knowledge of the specific value of the coupling constant (without loss of generality, it can be taken to be unity).

Our approach to the problem can be described as follows [Tokuda *et al.*, 2007]:

(1) Determine the phases $\theta_i(t)$ from the data $x_i(t)$. Among various definitions of phases [Pikovsky *et al.*, 2001], a simple formula is chosen, where the phase θ is increased by 2π at every local maximum of $x(t)$, and between the local maxima the phase grows proportionally in time.
(2) Fit the phases $\{\theta_i(t)\}$ to the phase equations:

$$\dot{\theta}_i = \omega_i + \frac{C}{N}\sum_{j=1}^{N} \tilde{H}(\theta_j - \theta_i), \tag{18}$$

where the interaction function $\tilde{H}$, which is in general nonlinear and periodic with respect to 2π, is approximated by a Fourier expansion up to order of D as $\tilde{H}(\Delta\theta) = \sum_{j=1}^{D} a_j \sin j\Delta\theta + b_j(\cos j\Delta\theta - 1)$.

The unknown parameters $p = \{\omega_i, a_j, b_j\}$ are estimated by the multiple-shooting method [Baake *et al.*, 1992]. We denote the time evolution of the phase equations (18) with respect to the initial condition $\theta(0)$ by $\theta(t) = \phi^t(\theta(0), p)$. Then, at each sampling time $t = i\Delta t$, the phase equation must satisfy the boundary conditions: $\theta((n+1)\Delta t) = \phi^{\Delta t}(\theta(n\Delta t), \mathbf{p})$. With respect to the unknown parameters p, we solve these nonlinear equations by the generalized Newton method, and we integrate the evolution function ϕ^t numerically. For the computation of the gradients $\partial\phi/\partial p$, which are needed for the Newton method, variational equations of the phase equations (18) are also solved numerically.

A necessary condition to solve the nonlinear equations is that the number of unknown parameters is less than the number of equations, corresponding in this case to $N + 2D < N(M - 1)$. This always holds in the case of enough data M.
(3) To avoid over-fitting, a cross-validation technique is used to determine the optimum number of higher harmonics in the interaction function, D [Stone, 1974]. We divide the multivariate data into two parts. For the first half of the data, the parameter values p are estimated, then we apply the estimated parameters to the latter half data and measure the error $E = \sum_n |\theta((n+1)\Delta t) - \phi^{\Delta t}(\theta(n\Delta t), \mathbf{p})|^2$. The order number D giving rise to the minimum error is considered to be the optimum.

4. Coupled Repressilator Model

We apply the technique described in the previous section to the genetic oscillator, which models the repressilator. The voltage V_1 of each oscillator is connected to a common point through a resistor R_c. We obtain this way a global coupling of the system, which is described by Eqs. (13)–(15) with

a multiplicative coefficient:

$$R_2C_2\frac{dV_2}{dt} = -\alpha_i V_2 + \alpha_i V_{cc} f(V_1), \tag{19}$$

$$R_3C_3\frac{dV_3}{dt} = -\alpha_i V_3 + \alpha_i V_{cc} f(V_2), \tag{20}$$

$$R_1C_1\frac{dV_1}{dt} = -\alpha_i V_1 + \alpha_i V_{cc} f(V_3) + R_1\frac{1}{R_c}\frac{1}{N}\sum_{n=0}^{N}(V_1^n - V_1). \tag{21}$$

Each unit gives rise to a limit cycle oscillation under the chosen parameter configuration without coupling $C = 0$. To consider inhomogeneity in the network, parameter values α_i are varied among the cells, and the multivariate data are recorded as $\{V_{i,2}(t)\}_{i=1}^{N}$.

Here, we examine the case of $N = 16$. Inhomogeneous parameter values were set as $\alpha_i = 1 + 0.005\cdot(i - 8.5)$ $(i = 1, 2, \ldots, 16)$. The data $\{V_{i,2}(t)\}_{i=1}^{16}$ were collected with the coupling strength $C = 0.01$, which gives rise to a nonsynchronized dynamics. The sampling interval was set to be $\Delta t = 0.08$ for the extraction of the phase $\{\theta_i(t)\}$. Then, by applying the multiple-shooting method the data have been down sampled to $\Delta t = 1000{\cdot}0.08$ and the total of 2000 data points have been collected for the parameter estimation. (As an initial condition, unknown parameter values are all set to be zero, i.e. $\omega_i = 0, a_j = b_j = 0$.) The convergence property of the multiple-shooting was excellent; a single Newton procedure gives a good estimate.

Figures 3(a) and 3(b) show the estimated interaction function and the natural frequencies of the uncoupled oscillators with the Fourier order of $D = 4$, which was optimized by the cross-validation test. The estimated natural frequencies are distributed on a diagonal line with the original frequencies computed from each of the repressilators. Moreover, the estimated interaction function $\tilde{H}(\Delta\theta)$ is in a very good agreement with that estimated by applying the perturbation method [Kuramoto, 1984; Sakaguchi *et al.*, 1987] to a single repressilator model.

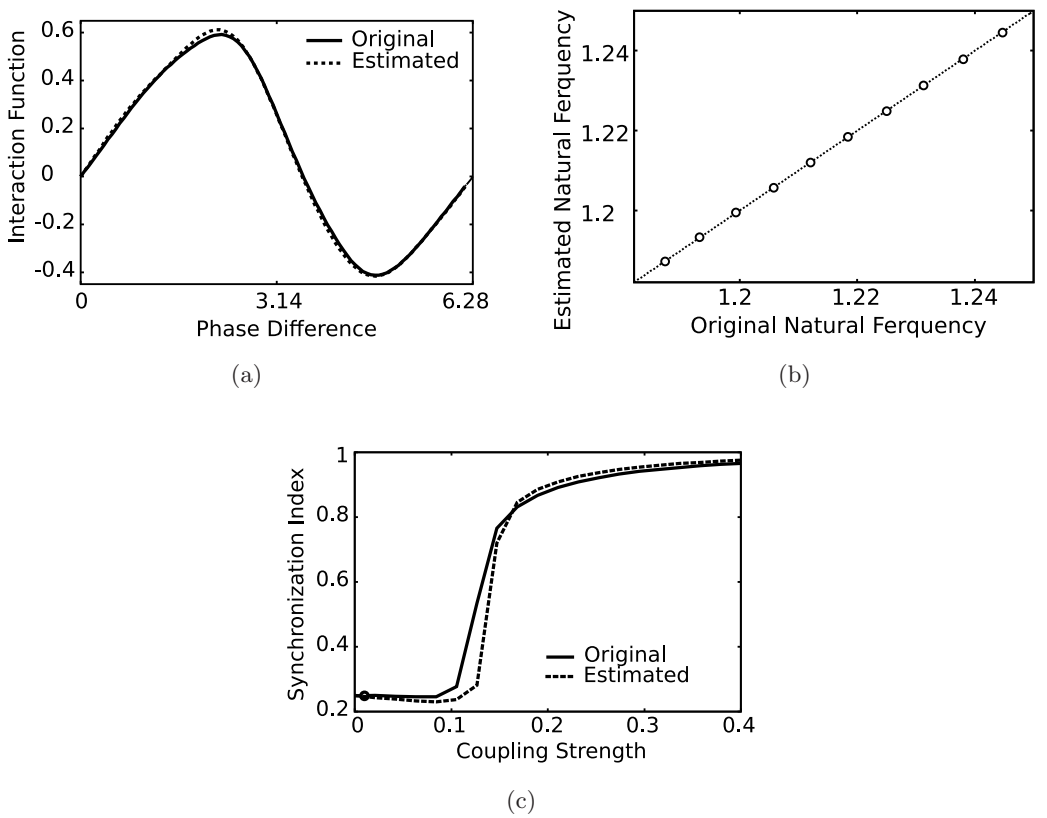

Fig. 3. Results of modeling the simulated data at $K = 0.01$. (a) Interaction function $\tilde{H}(\Delta\theta)$ estimated by the perturbation method (solid line) and by the present method (dotted line). (b) Natural frequencies of the original system against its estimation. (c) Synchronization diagram of the original system (solid line) and estimation (dotted line). Circle point corresponds to the coupling strength used for the modeling.

The estimated phase model (18) can be used for predicting the synchronization structure. Figure 3(c) shows the dependence of the order parameter Φ on the coupling strength, where Φ was computed according to $Re^{i\Phi} = 1/N\sum_{j=1}^{N} e^{i\phi_j}$ (ϕ_j: phase of jth cell). The phase model gives an excellent prediction of the order versus coupling strength curve. The Kuramoto transition point [Kuramoto, 1984] (onset of synchronization) observed in the original repressilator model (19)–(21) is predicted by the phase model, even though only a single data point is used for the parameter estimation.

We remark that this precision of predictability is expected as far as the coupling strength is weak enough. Under such a weak coupling, the phase reduction theory guarantees that the phase dynamics is invariant [Kuramoto, 1984]. This is essential for predicting the onset of synchronization from a weaker coupling regime. In contrast, if the synchronization takes place only at a very strong coupling, the phase dynamics gets distorted. In that case, it becomes more difficult to predict the synchronization. In that sense, there is a certain limitation of predicting the onset of synchronization.

It is important to note that the estimation results depend on the modeling condition. Figures 4(a)–4(c) show the dependence of the estimation error on the data length M, observational noise, and percentage of the number of observed repressilators. The estimation error was measured as a deviation of the estimated interaction function $\tilde{H}_s(\Delta\theta)$ from the one $\tilde{H}_p(\Delta\theta)$ estimated by the perturbation method, i.e. $E = \int_0^{2\pi} \|\tilde{H}_s(\Delta\theta) - \tilde{H}_p(\Delta\theta)\| d\Delta\theta$. As the observational noise, independent zero-mean Gaussian noise $\xi \in N(0, \gamma^2)$ was added to each of the multivariate data $\{V_{i,2}(t)\}_{i=1}^{16}$, where the noise level is given by $100\gamma/\sigma$ [%] (σ: standard deviation of the signal V). The percentage of the number of observed oscillators is given by $100N/16$ [%], where only a subset of N measurements $\{V_{i,2}(t)\}_{i=1}^{N}$ was used among the 16 measurements $\{V_{i,2}(t)\}_{i=1}^{16}$.

As shown in Fig. 4(a), the data length of $M = 100$ is required for a precise estimation of the interaction function. Since the sample interval of this study was set to be relatively long ($\Delta t = 1000 \cdot 0.08$), the total number of oscillation cycles included within these data ($M = 100$) were about 1600. Sometimes, this amount of oscillation cycles

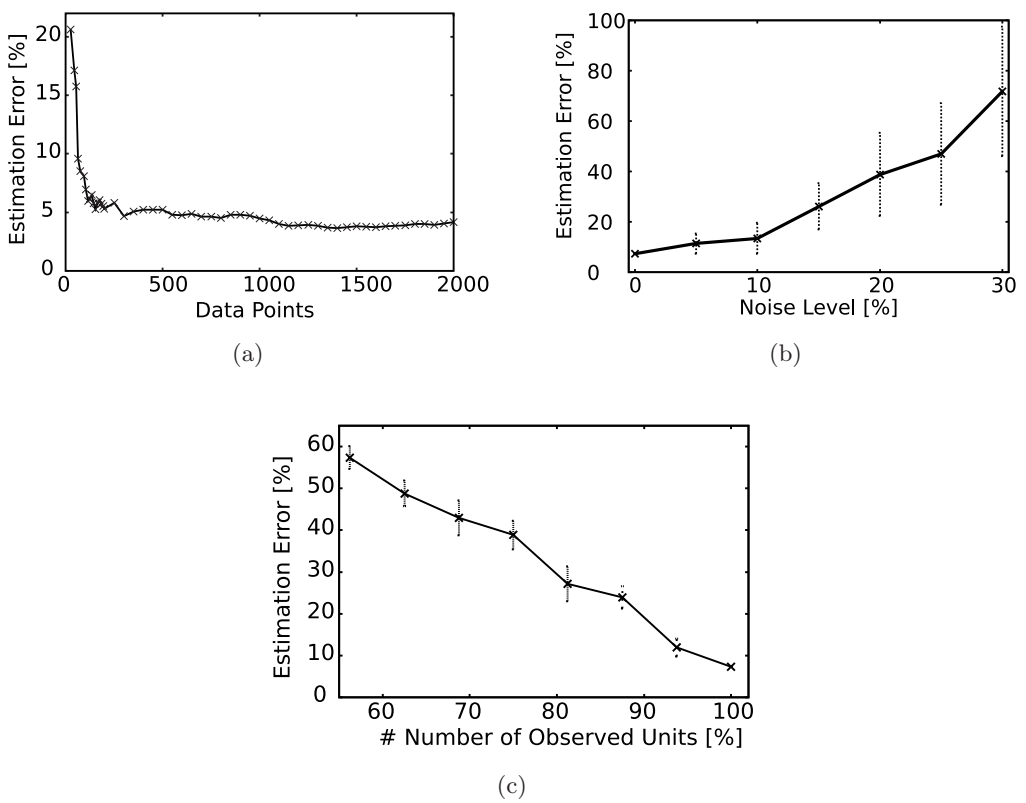

Fig. 4. (a) Dependence of the estimation error on the data number. (b) Dependence of the estimation error on the observational noise. (c) Dependence of the estimation error on the percentage of the number of observed repressilators.

cannot be recorded from the experiment. According to another simulation using much shorter sampling interval ($\Delta t = 40{\cdot}0.08$), the data length of $M = 120$ was found to be enough for a precise estimation, where the number of oscillation cycles within this data was about 80. This amount of cycles can be expected for normal experimental data.

Figure 4(b) shows the influence of the observational in the case that the data length is fixed to $M = 80$. The estimation is found to be robust up to the observational noise of 10%, which is practical for a real experimental situation. Although the estimation result is rather sensitive to the percentage of the observed cells, it still provides a good estimate even if 5% of the cells is not observed.

5. Application to Electronic Circuit Data

Our technique has been finally applied to experimental data measured from electronic genetic networks with 16 coupled units [Wagemakers *et al.*, 2006]. In this section we contrast the result obtained with the numerical algorithm and the experiments.

In order to compare the numerical algorithm with the experiment, the interaction function $\tilde{H}$ of the coupled system must be estimated. This function can be estimated with the help of the phase response curve.

The phase response curve represents the phase displacement of the oscillator when a perturbation is applied during the cycle [Winfree, 1980]. To elaborate this curve, small perturbations are applied at different times of the cycle. In our case these perturbations are short electric pulses. The phase displacement is compared with the phase previous to the shock. The phase shift is represented in function of the phase of the cycle. Figure 5(a) represents the experimental phase response curve along with the waveform of the oscillator.

The interaction function $\tilde{H}$ for weak coupling can be estimated from the experimental phase

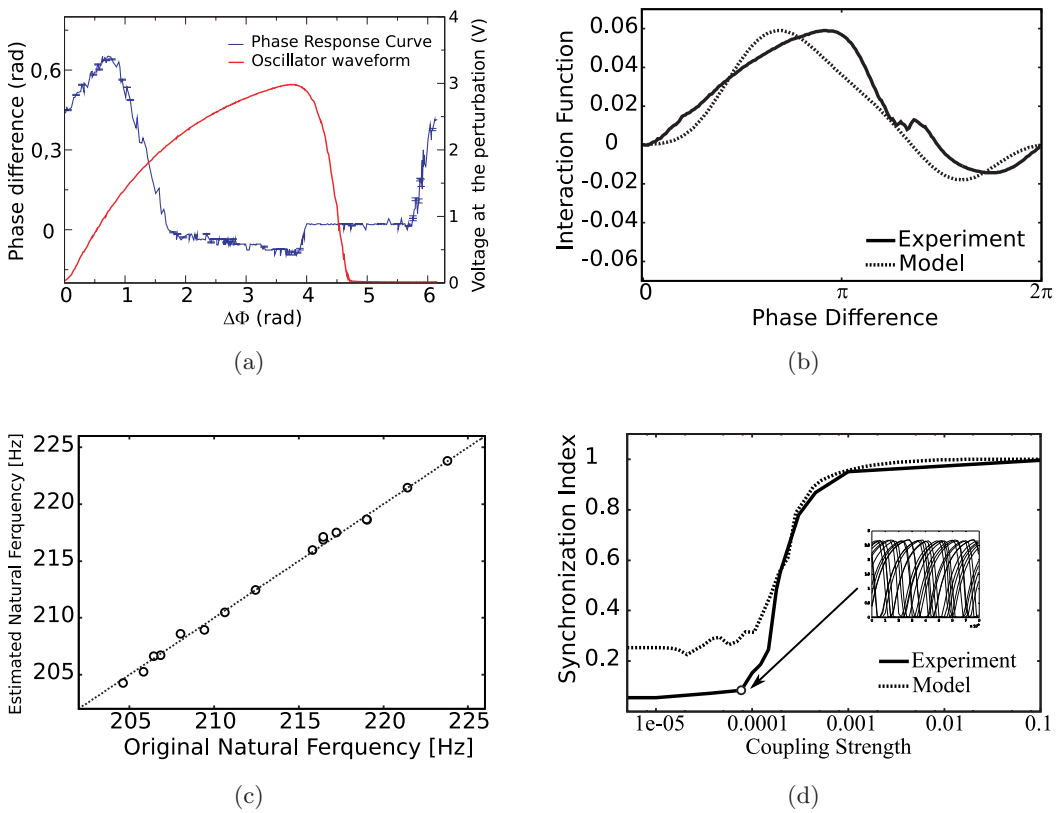

Fig. 5. (a) Phase response curve of a single circuit along with the waveform of the oscillation. (b) Interaction function $\tilde{H}(\Delta\theta)$ of the experimental system (solid line) and its estimate (dotted line). (c) Natural frequencies of the experimental system against its estimate. (d) Synchronization diagram of experimental system (solid line) and estimate (dotted line). Circle point corresponds to the coupling strength used for the modeling. In the inset graphic the time series of the circuit for the weak coupling configuration is shown for the coupling $R_c = 13\,\mathrm{k}\Omega$.

response curve [Kuramoto, 1984]. The measured interaction function of the circuit is represented in Fig. 5(b). The interaction function is also computed from a time series of the experiments in a weak coupling regime. Despite some differences between the numerical algorithm and the experiment in Fig. 5(b), the results are consistent. Figure 5(b) shows the estimated natural frequencies of the oscillators. The Fourier order was optimized by the cross-validation test as $D = 3$. The last figure represents the estimated synchronization diagram compared to the experimental measurements. Note that the computed diagram has been obtained from a single time series of the weak coupled system. The time series is circled in red in Fig. 5(d). The transition to synchrony is very well represented in this graphic. The results validate the assumption that the system can be estimated by a set of coupled phase oscillators when the coupling between units is weak.

6. Conclusions

A phase model has been estimated from an experimental data of an electronic genetic network. The estimation technique requires only a single set of multivariate data recorded simultaneously from all units of the genetic oscillators. The estimation accuracy has been checked by comparing the estimated interaction function with the one obtained by the perturbation method. The estimated phase model was further utilized to study the dependence of the synchronized state of genetic oscillators on the coupling strength. The phase model was shown to be capable of recovering the route from non-synchronization to synchronization with an accurate onset point, which agrees quite well with the experiment.

The next challenge of the present approach is to apply it to experimental data from synthetic biological system such as coupled synthetic genetic oscillators. Experimental realization of the coupling among such synthetic oscillators is awaited. To deal with biological data, the dynamical noise should be an important issue, since biological systems are inherently noisy. We believe that the present approach might be robust against a moderate amount of dynamical noise as shown by its application to the electronic data, which includes a certain amount of dynamical noise. However, in the case that a strong level of dynamical noise exists, the phase dynamics should take the form of stochastic differential equations. To deal with such stochastic dynamics, the parameter estimation technique should be modified such as using the averaging method [Siegert *et al.*, 1998]. Such approach to deal with the dynamical noise will be considered in our future work.

Acknowledgments

Financial support from the Ministry of Education and Science (Spain) under Project No. FIS2006-08525 by the Spanish Ministry of Science and Innovation under Project No. FIS2009-09898 and from the Ministry of Education, Science, Sports, and Culture (Japan) under Grants-in-Aid for Scientific Research (C) (No. 20560352) is acknowledged.

References

Baake, E., Baake, M., Bock, H. G. & Briggs, K. M. [1992] "Fitting ordinary differential equations to chaotic data," *Phys. Rev. A* **45**, 5524.

Elowitz, M. B. & Leibler, S. [2000] "A synthetic oscillatory network of transcriptional regulators," *Nature* **403**, 335.

Elson, R. C., Selverston, A. I., Huerta, R., Rulkov, N. F., Rabinovich, M. I. & Abarbanel, H. D. I. [1998] "Synchronous behavior of two coupled biological neurons," *Phys. Rev. Lett.* **81**, 5692.

Galan, R. F., Ermentrout, G. B. & Urban, N. N. [2005] "Efficient estimation of phase-resetting curves in real neurons and its significance for neural-network modeling," *Phys. Rev. Lett.* **94**, 158101.

García-Ojalvo, J., Elowitz, M. B. & Strogatz, S. [2004] "Modeling a synthetic multicellular clock: Repressilators coupled by quorum sensing," *Proc. Natl. Acad. Sci. USA* **101**, 10955.

Kiss, I. Z., Zhai, Y. M. & Hudson, J. L. [2005] "Predicting mutual entrainment of oscillators with experiment-based phase models," *Phys. Rev. Lett.* **94**, 248301.

Kori, H. & Mikhailov, A. S. [2004] "Entainment of randomly coupled oscillator networks by a pacemaker," *Phys. Rev. Lett.* **93**, 254101.

Kuramoto, Y. [1984] *Chemical Oscillations, Waves and Turbulence* (Springer, Berlin).

McClintock, M. [1971] "Menstrual synchrony and suppression," *Nature* **229**, 244.

Miyazaki, J. & Kinoshita, S. [2006] "Determination of a coupling function in multicoupled oscillators," *Phys. Rev. Lett.* **96**, 194101.

Pikovsky, A., Rosenblum, M. & Kurths, J. [2001] *Synchronization — A Universal Concept in Nonlinear Sciences* (Cambridge University Press, Cambridge).

Sakaguchi, H., Shinomoto, S. & Kuramoto, Y. [1987] "Local and global self-entrainment in oscillator lattices," *Progr. Theoret. Phys.* **77**, 1005.

Siegert, S., Friedrich, R. & Peinke, J. [1998] "Analysis of data sets of stochastic systems," *Phys. Lett. A* **243**, 275.

Stone, M. [1974] "Cross-validatory choice and assessment of statistical predictions," *J. Royal Stat. Soc. B* **36**, 111.

Tokuda, I. T., Jain, S., Kiss, I. Z. & Hudson, J. L. [2007] "Inferring phase equations from multivariate series," *Phys. Rev. Lett.* **99**, 064101.

Wagemakers, A., Buldú, J. M., García-Ojalvo, J. & Sanjuán, M. A. F. [2006] "Synchronization of electronic genetic networks," *Chaos* **16**, 013127.

Winfree, A. T. [1980] *The Geometry of Biological Time* (Springer, NY).

Yamaguchi, S., Isejima, H., Matsuo, T. & Okura, R. [2003] "Synchronization of cellular clocks in the suprachiasmatic nucleus," *Science* **302**, 1408.